

A measurable force driven by an excitonic condensate

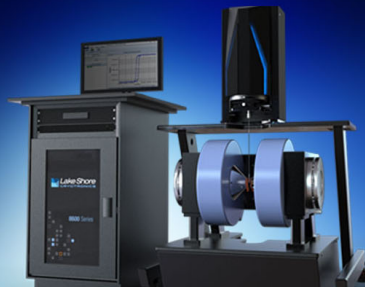
T. Hakioglu, Ege Özgün, and Mehmet Günay

Citation: *Appl. Phys. Lett.* **104**, 162105 (2014);

View online: <https://doi.org/10.1063/1.4873377>

View Table of Contents: <http://aip.scitation.org/toc/apl/104/16>

Published by the [American Institute of Physics](#)



8600 Series VSM

For fast, highly sensitive
measurement performance

LEARN MORE 

A measurable force driven by an excitonic condensate

T. Hakioglu,^{1,2} Ege Özgün,¹ and Mehmet Günay¹

¹Department of Physics, Bilkent University, 06800 Ankara, Turkey

²Institute of Theoretical and Applied Physics, 48740 Turunç, Muğla, Turkey

(Received 2 January 2014; accepted 15 April 2014; published online 23 April 2014)

Free energy signatures related to the measurement of an emergent force ($\approx 10^{-9}$ N) due to the exciton condensate (EC) in Double Quantum Wells are predicted and experiments are proposed to measure the effects. The EC-force is attractive and reminiscent of the Casimir force between two perfect metallic plates, but also distinctively different from it by its driving mechanism and dependence on the parameters of the condensate. The proposed experiments are based on a recent experimental work on a driven micromechanical oscillator. Conclusive observations of EC in recent experiments also provide a strong promise for the observation of the EC-force.

© 2014 AIP Publishing LLC. [<http://dx.doi.org/10.1063/1.4873377>]

In the late 1940s, Casimir predicted an unusual force between two neutral metallic plates held in vacuum.¹ The Casimir Force (CF) is attractive between the two ideally infinite metallic plates and the Casimir pressure is given by $P_c = \mathcal{F}_c/A = -\pi^2\hbar c/(240D^4)$ where A is the area of the plates and D is the separation between them. For typical values $A \simeq 1 \mu\text{m}^2$ and $D \simeq 100 \text{ \AA}$, $\mathcal{F}_c \simeq -1.3 \times 10^{-7}$ N. The early measurements of CF were done between a metal plate and a metal sphere.² Twelve years ago perfect agreement with the theory was achieved for the original two plate geometry.^{3,4}

Vacuum is the lowest energy (ground) state of the electromagnetic radiation with zero field strength and nonzero fluctuations. The electromagnetic field is defined by the excitations of the electromagnetic modes above the vacuum. This perception will be useful here where the vacuum is the ground state of a many body interacting excitonic system in the condensed state. The vacuum of the free electromagnetic radiation is smoothly connected with its excitation spectrum and can be reached perturbatively by changing the number of excited modes and other physical parameters. Same thing is also true for the binary liquid mixtures in the critical regime. A force similar to the universal CF, i.e., the Critical Casimir Force (CCF) has been predicted⁵ and measured⁶ in these systems. On the other hand, in many body interacting systems, there are also nonperturbative ground states that can have a finite energy gap in the excitation spectrum. The existence of the finite gap, away from the critical point where the gap vanishes, can prevent small fluctuations at zero temperature. Close to the critical point however, there are predictions of the CCF in Bose-Einstein condensates (BEC),⁷ but this has not been experimentally verified yet. On the other hand, the Casimir-Polder-like force between a BEC and a semiconductor plane was measured.⁸ In condensed systems with a finite energy gap away from the critical point at sufficiently small temperatures, one may therefore expect that Casimir like effects are strongly suppressed and may not be observed.

The starting point to generalize Casimir's concept here is the dependence of the free energy on the system's boundaries which may be realized in two different ways. One is the Dirichlet or von-Neumann type boundary conditions affecting the critical fluctuations of the order parameter leading to

the Casimir-like phenomena discussed above. The second is the strength of the order parameter, and hence the energy gap itself, depending on system's size through the pairing interaction. Here, we concentrate on the latter taking the example of a low temperature condensate of which the pairing strength depends on the physical size, i.e., the spatially indirect Coulomb coupling between electrons and holes confined to two separate quantum wells (the Double Quantum Well (DQW) geometry) as given by $v_{eh}(\mathbf{r}) = -e^2/(4\pi\epsilon\sqrt{\mathbf{r}^2 + D^2})$ where $\mathbf{r} = (\mathbf{r}_e - \mathbf{r}_h)$, \mathbf{r}_e and \mathbf{r}_h are the electron-hole (eh) coordinates, D is the separation between the quantum wells, and ϵ is the dielectric constant. There are two effects of $v_{eh}(\mathbf{r})$. If D is on the order of an exciton Bohr radius a_B (about 100 Å for GaAs based materials), the first effect is the formation of Wannier Mott excitons. Below a certain critical temperature T_c , the second effect comes into play. In sufficiently low exciton densities n_x , when excitons act like independent bosons, they are expected to Bose-Einstein condense⁹ with an energy gap depending on the strength of the Coulomb coupling. As n_x increases, the excitons start spatially overlapping, with a higher Fermi energy scale than the pairing interaction, moving into a BCS like condensed ground state. This work is focused on the second effect of the Coulomb interaction.

In an exciton condensate (EC), two different types of pairings¹⁰ are allowed between an electron in an s-like and a hole in a p-like orbital. The bright pairs have opposite eh spins forming bright singlets and bright triplets, whereas the dark triplet has parallel eh spins. The bright states can couple to the radiation field through the recombination and pair creation due to their odd total angular momenta, whereas the dark states do not. However, in reality, the dark and the bright states are mixed.¹⁰⁻¹² Two dark states can turn into two bright ones by exchanging their electrons or holes within their proper quantum wells (the Pauli exchange).¹³ Therefore, there is always a weak bright component in the ground state by which the photoluminescence experiments can be made. Until recently, these experiments have been inconclusive in probing the EC due to the weakness of the bright contribution.¹⁴ Recently, a clear evidence was established¹⁵ by the observation of the interference fringes due to the condensate's macroscopic wavefunction.

The condensation free energy (CFE) does not differentiate between the dark and the bright components and hence, offers a promising path in providing additional support to the photoluminescence measurements.¹⁵ In these systems, the CFE depends on the layer separation D through the condensate's order parameter. For smaller D , the attractive coupling is stronger and the CFE is lower, pointing at an attractive force between the electron and hole rich quantum wells. This force, which we may coin as the EC-force, is driven by the Coulomb interaction but is only present due to the condensate. We address here three fundamental questions: (1) Can we understand the analytic dependence of the EC-force on the physical parameters?, (2) Is the EC-force measurable under realistic conditions and current experimental accuracy?, and (3) If so, how can we measure it?

The microscopic Hamiltonian is our starting point given in the eh basis ($\hat{e}_{\mathbf{k}\uparrow}\hat{e}_{\mathbf{k}\downarrow}\hat{h}_{-\mathbf{k}\uparrow}^\dagger\hat{h}_{-\mathbf{k}\downarrow}^\dagger$) at a fixed momentum $\mathbf{k} = (k_x, k_y)$ by

$$\mathcal{H}_\Delta = \sum_{\mathbf{k}} \left\{ \begin{pmatrix} \epsilon_{\mathbf{k}}\sigma_0 & \bar{\Delta}_{\mathbf{k}}^\dagger \\ \bar{\Delta}_{\mathbf{k}} & -\epsilon_{\mathbf{k}}\sigma_0 \end{pmatrix} + \epsilon_{\mathbf{k}}^{(-)}\sigma_0 \otimes \sigma_0 \right\}, \quad (1)$$

where σ_0 is the 2×2 unit matrix, $\bar{\Delta}_{\mathbf{k}}$ is the 2×2 matrix describing the self-consistent and spin dependent order parameter $\Delta_{\sigma\sigma'}(\mathbf{k})$ with $\sigma, \sigma' = \{\uparrow, \downarrow\}$ as the spin indices, $\epsilon_{\mathbf{k}} = (\zeta_{\mathbf{k}}^{(e)} + \zeta_{\mathbf{k}}^{(h)})/2$ and $\epsilon_{\mathbf{k}}^{(-)} = (\zeta_{\mathbf{k}}^{(e)} - \zeta_{\mathbf{k}}^{(h)})/2$ are the single particle energies in terms of the electron and hole single particle energies $\zeta_{\mathbf{k}}^{(e)} = \hbar^2\mathbf{k}^2/(2m_e) - \mu_e$ and $\zeta_{\mathbf{k}}^{(h)} = \hbar^2\mathbf{k}^2/(2m_h) - \mu_h$ parameterized by the electron and the hole band masses m_e, m_h , and the respective chemical potentials μ_e, μ_h . We assume that $m_e = m_h$,¹⁶ whereas allow, for now, an imbalance between their concentrations. We have then, $\epsilon_{\mathbf{k}}^{(-)} = -\mu_-$ where $\mu_- = (\mu_e - \mu_h)/2$.

The order parameter in Eq. (1) is given by

$$\Delta_{\sigma\sigma'}(\mathbf{k}) = -\frac{1}{2A} \sum_{\mathbf{k}'} V_{eh}(\mathbf{k} - \mathbf{k}') \langle \hat{e}_{\mathbf{k}'\sigma}^\dagger \hat{h}_{-\mathbf{k}'\sigma'}^\dagger \rangle, \quad (2)$$

where A is the sample area and $V_{eh}(\mathbf{q}) = -e^{-qD}e^2/(2\epsilon q)$ is the Fourier transform of $v_{eh}(\mathbf{r})$ with $q = |\mathbf{k} - \mathbf{k}'|$ as the eh exchange momentum. The pairing strength is $\langle \hat{e}_{\mathbf{k}\sigma}^\dagger \hat{h}_{-\mathbf{k}\sigma'}^\dagger \rangle = \Delta_{\sigma\sigma'}(\mathbf{k})/(2E_{\mathbf{k}})[f_+(\mathbf{k}) - f_-(\mathbf{k})]$ and $f_\nu(\mathbf{k}) = 1/(1 + e^{\beta\lambda_{\nu,\mathbf{k}}})$ is the Fermi-Dirac factor with $\beta = 1/k_B T$, with T as the temperature. The energy bands of Eq. (1) are time reversal degenerate,^{10,12} with $\nu = (+, -)$ denoting the doubly degenerate upper and the lower excitonic branches. Here, $\lambda_{\nu,\mathbf{k}} = \epsilon_{\mathbf{k}}^{(-)} + \nu E_{\mathbf{k}}$ are the eigenenergies, $E_{\mathbf{k}} = \sqrt{\epsilon_{\mathbf{k}}^2 + \Delta_{\mathbf{k}}^2}$ and $\Delta_{\mathbf{k}} = (|\Delta_{\uparrow\uparrow}|^2 + |\Delta_{\uparrow\downarrow}|^2)^{1/2}$.

Equation (2), together with the self energies, constraints on the particle number conservation and the coupling of the bright states to the radiation field, have been numerically solved in Ref. 12 with an observation that the radiation field strongly suppresses the bright contribution, i.e., $|\Delta_{\uparrow\downarrow}| \ll |\Delta_{\uparrow\uparrow}|$ which implies that the condensate is dominated by the dark states, i.e., $\Delta_{\mathbf{k}} \simeq |\Delta_{\uparrow\uparrow}(\mathbf{k})| = |\Delta_{\downarrow\downarrow}(\mathbf{k})|$.

The second observation was the presence of a sharp phase boundary determined by n_x, n_- , and D between the condensed

phase and the incoherent excitonic liquid determined by $\Delta_{\mathbf{k}}(T, n_x, n_-, D) = 0$. At $T = 0$, the numerical solution of $\Delta_{\mathbf{k}}$ resembles the shape of an inverted parabola (Fig. (3) in Ref. 12) as a function of $D_c - D$ near $D \simeq D_c$ where D_c is the critical layer separation for fixed n_x and n_- . Our first goal here is to understand this behavior analytically and calculate the CFE from which an analytic expression is obtained for the EC-force.

The CFE is given by $\Delta\Omega = \Omega_\Delta - \Omega_0 \leq 0$. Here, Ω_Δ and Ω_0 are the total free energies in the condensed and the uncondensed phases, respectively. In an EC, we observe two types of dependence on D . The first is the critical thermal fluctuations of the condensate near T_c . This term is suppressed if $T \ll T_c$. The second dependence on D arises from $\Delta_{\mathbf{k}}$ which is essential for the results in this work. On the other hand, the electron and hole self energies are driven by D -independent interactions.

The EC-force is given by

$$\mathcal{F}_{EC} = -\sum_{\mathbf{k}} \frac{\delta\Delta\Omega}{\delta\Delta_{\mathbf{k}}} \frac{\partial\Delta_{\mathbf{k}}}{\partial D}, \quad (3)$$

where Ω_Δ , up to a $\Delta_{\mathbf{k}}$ independent constant, is

$$\Omega_\Delta = \sum_{\nu,\mathbf{k}} \left\{ \nu f_\nu(\mathbf{k}) \frac{\Delta_{\mathbf{k}}^2}{(2E_{\mathbf{k}})} - \frac{\partial}{\partial\beta} \ln(1 - f_\nu(\mathbf{k})) \right\}. \quad (4)$$

Equation (4) reduces, at $T = 0$ and $\epsilon_{\mathbf{k}}^{(-)} = 0$, to the standard expression $\Omega_\Delta = -\sum_{\mathbf{k}} \{\Delta_{\mathbf{k}}^2/(2E_{\mathbf{k}}) + E_{\mathbf{k}}\}$.

In the light of the previous discussions and at $T = 0$, Eq. (2) reduces to a single gap equation¹²

$$\Delta_{\mathbf{k}} = -\frac{\pi e^2}{\epsilon} \int \frac{d\mathbf{q}}{(2\pi)^2} \frac{e^{-qD}}{q} G_{\mathbf{k}+\mathbf{q}}, \quad (5)$$

where $G_{\mathbf{k}} = \Delta_{\mathbf{k}} F_{\mathbf{k}} / \sqrt{(\epsilon_{\mathbf{k}} - \mu_x)^2 + \Delta_{\mathbf{k}}^2}$ and

$$\lim_{k \rightarrow 0} F_{\mathbf{k}} = \begin{cases} 1 & \text{for } \Delta_0^2 + \mu_x^2 < \mu_-^2 \\ -1 & \text{for } \Delta_0^2 + \mu_x^2 > \mu_-^2 \end{cases}. \quad (6)$$

The first case in Eq. (6) is allowed when there is a high eh imbalance, indicated by a sufficiently large μ_- . In this case, no non-zero solution of Eq. (5) exists, which is consistent with Ref. 12. If μ_- is weak or zero, a nonzero solution is allowed by the lower case in Eq. (6). Considering $\mu_- = 0$ the particle number conservation becomes

$$n_x = \frac{1}{A} \sum_{\mathbf{k}} \left(1 - \frac{\epsilon_{\mathbf{k}}}{E_{\mathbf{k}}} \right), \quad (7)$$

which determines μ_x . An exact solution of Eqs. (5) and (7) is not possible due to the presence of the momentum dependent interaction $V_{eh}(\mathbf{q})$. Our motivation here is to resort to a proper approximation which can be done near the phase boundary. We also show below that this solution reproduces the basic results of Ref. 12.

The exponential term e^{-qD} in Eq. (5) hints for a proper approximation implying that the leading contribution comes from $q \ll 1/D$. Expanding $G_{\mathbf{k}+\mathbf{q}}$ up to second order in q near $q = 0$, we have $G_{\mathbf{k}+\mathbf{q}} \simeq G_{\mathbf{k}} + \nabla_{\mathbf{k}} G_{\mathbf{k}} \cdot \mathbf{q} + G_{\mathbf{k}}'' q^2/2$. Here, $G_{\mathbf{k}}''$ is

the second derivative of G_{k+q} at $q=0$. In both expansions, the first order terms in momentum are absent due to the angular symmetry. Using these in Eq. (5), we have a self consistency condition for $\Delta_0 = \Delta_{\mathbf{k}}|_{\mathbf{k}=0}$ and $\Delta_0'' = \Delta_{\mathbf{k}}''|_{\mathbf{k}=0}$ given by

$$\Delta_0 = \sqrt{E_0^2 - \mu_x^2}, \quad \Delta_0'' = -\frac{\Delta_0 \hbar^2}{\mu_x m}, \quad E_0 = \frac{e^2}{2\epsilon D}, \quad (8)$$

yielding $\Delta_{\mathbf{k}} = -\Delta_0 \epsilon_{\mathbf{k}}/\mu_x$. The quasiparticle eigenenergies can then be simply expressed as $E_{\mathbf{k}} = \sqrt{\epsilon_{\mathbf{k}}^2 + \Delta_{\mathbf{k}}^2} = E_0 |\epsilon_{\mathbf{k}}|/\mu_x$. Equation (8) is an indication that the model can reproduce the sharp phase boundary with the critical layer separation $D = D_c$ given by $D_c = e^2/(2\epsilon\mu_x)$ where, using the parabolic approximation in Eq. (7)

$$\mu_x = -\frac{E_0}{2} + \sqrt{\left(\frac{E_0}{2}\right)^2 + \frac{E_0 n_x}{\Gamma}}, \quad (9)$$

with $\Gamma = m_x/(2\pi\hbar^2)$ being the two-dimensional density of states with m_x as the exciton reduced mass. Eqs. (8) and (9) can be used to find $\Delta\Omega$ in Eq. (4). Expansion of Eq. (8) near $D = D_c$ yields the sharp phase boundary as

$$\Delta_0 \simeq \alpha \sqrt{1 - \frac{D}{D_c}} \quad \text{with} \quad \alpha = \sqrt{\frac{4}{3}} E_0, \quad (10)$$

which is valid for $D \leq D_c$. The $\Delta\Omega$ given by Eq. (4) can be found similarly using Eqs. (8) and (9) as

$$\Delta\Omega = -\frac{\Gamma}{E_0} \left[\mu_x \left(\mu_x^2 + \frac{3}{2} \Delta_0^2 \right) - \mu_0^3 \right], \quad D \leq D_c, \quad (11)$$

where $\mu_0 = n_x/2\Gamma$ is the chemical potential μ_x evaluated at the phase boundary $\Delta_0 = 0$. Using Eqs. (9) and (10), Eq. (11) can be represented at the phase boundary as

$$\Delta\Omega = -3\Gamma\mu_0^2 \left(1 - \frac{D}{D_c} \right), \quad D \simeq D_c, \quad (12)$$

predicting a linear dependence with respect to D ($\Delta\Omega = 0$ for $D_c < D$). A comparison between Ref. 12 in the vicinity of the phase boundary and Eqs. (10) and (12) are shown in Fig. 1. The accuracy of the parabolic approximation in capturing the main features of the numerical calculations in Ref. 12 is quite remarkable. Encouraged by this, now we proceed to the main result of our work, i.e., finding the EC-force. Using Eq. (12) in Eq. (3) we find that

$$\frac{\mathcal{F}_{EC}}{A} \simeq -\frac{3}{4} \frac{n_x^2}{\Gamma D_c}, \quad D \simeq D_c \quad (13)$$

with $\mathcal{F}_{EC} = 0$ for $D_c < D$. The Eq. (8) yields D_c as

$$\frac{a_B}{D_c} = \frac{2\epsilon\mu_0 a_B}{e^2} = \frac{n_x a_B^2}{2}. \quad (14)$$

For a sample size of $A \simeq 10^3 \mu\text{m}^2$ and a typical concentration of $n_x \simeq 3 \times 10^{11} \text{cm}^{-2}$, the EC-force is $\mathcal{F}_{EC} \simeq 10^{-9} \text{N}$ which is quite measurable within experimentally available precision. However, there is always the static Coulomb force

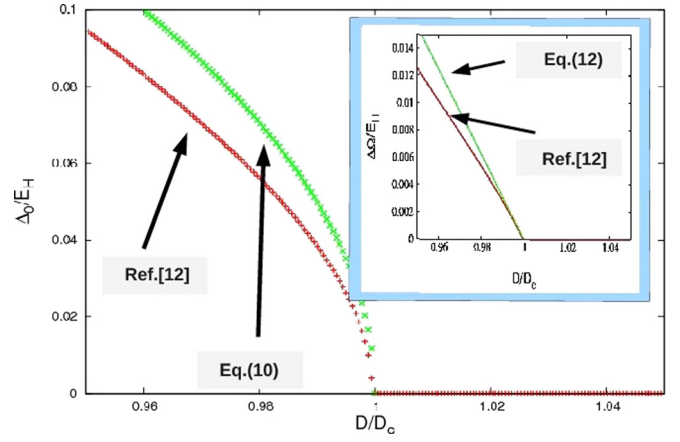


FIG. 1. Comparison of Ref. 12 with Eqs. (10) and (12) as D is varied near D_c . The main figure depicts Δ_0/E_H and the inset is $\Delta\Omega/E_H$, where $E_H = e^2/(4\pi\epsilon a_B)$ and $a_B = \hbar^2 4\pi\epsilon/(e^2 m_x)$. (The numerical solution includes the self energies as well as their realistically different masses.)

present independently from the condensate. One can compare \mathcal{F}_{EC} in the condensed phase with the Coulomb force \mathcal{F}_C between the quantum wells. Using Eq. (13) and $\mathcal{F}_C = e^2 n_x^2 A/\epsilon$ we have

$$\frac{\mathcal{F}_{EC}}{\mathcal{F}_C} = \begin{cases} 3a_B/(8D_c) & \text{for } D_c > D, \\ 0 & \text{for } D_c < D. \end{cases} \quad (15)$$

Considering $D \simeq 100 \text{\AA}$ and $n_x \simeq 3 \times 10^{11} \text{cm}^{-2}$, the two different regimes in Eq. (15) can be controlled by varying n_x . Note that $\mathcal{F}_C \propto n_x^2$, whereas $\mathcal{F}_{EC} \propto n_x^3$.

Here, we propose experiments for the measurement of \mathcal{F}_{EC} . Due to the dielectric between the quantum wells, the direct measurement is more challenging than measuring the CF between two metal plates in vacuum. Recently, Yamaguchi, Okamoto, Ishihara, and Hirayama have detected¹⁷ the motion of a micromechanical oscillator with an amplitude on the order of 50 nm. Upon this work, we use the EC-force as the driver of the micromechanical oscillator as shown in Fig. 2.

In order to measure \mathcal{F}_{EC} one has to subtract the \mathcal{F}_C as well as the external electric (E)-field.¹⁸ For this, we use a

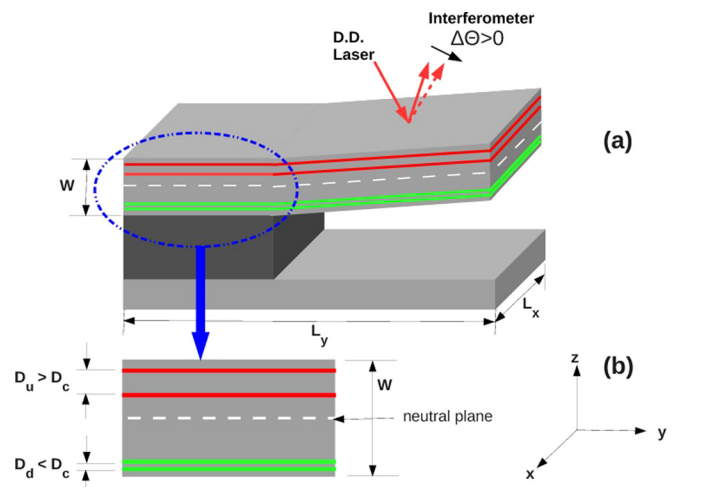


FIG. 2. The proposed mechanical resonator for the EC-force measurement via an interferometer and a DD laser. Here, (a) is the general set-up with physical dimensions, and (b) magnified view of the cross section with two DQWs.

two DQW geometry and that $\mathcal{F}_C = e^2 n_x^2 A / (2\epsilon)$ as well as the external force $\mathcal{F}_{ext} = eE_{ext}$ are independent of D .¹⁹ Specifically, two DQWs with slightly unequal layer separations $D_u \neq D_d$ are grown on either side of the neutral plane of the cantilever in Fig. 2. The D_u , D_d , and n_x are arranged such that one DQW is driven into the condensed phase, i.e., $D_d/D_c = 1 - \delta$, whereas the other is not, i.e., $D_u/D_c = 1 + \delta$, where $0 < \delta \ll 1$. The DQWs are driven by the same pump laser and are subject to the same external E-field. Using slightly different well widths, the exciton lifetime hence the equilibrium populations in both wells can be made comparable.²⁰ In this geometry, the \mathcal{F}_C as well as \mathcal{F}_{ext} in both DQWs are also comparable, whereas, the lower DQW has a nonzero \mathcal{F}_{EC} creating a net bending stress on the cantilever and driving the cantilever's motion as shown below.

Although static measurements can be performed with acceptable accuracy, the measurement of the periodically driven oscillations of the cantilever is more promising. A typical cantilever oscillator¹⁷ can be driven with a power consumption $P = m_{eff} \Omega_0^3 \Delta z_{rms}^2 / Q \simeq 2 \times 10^{-15} J/s$, where Δz_{rms} is the rms vibrational amplitude, $m_{eff} \simeq 10^{-10} \text{ kg}$ is the effective mass of the cantilever, $\Omega_0 / (2\pi) \simeq 20 \text{ kHz}$ is the resonance frequency, and $Q \simeq 2.5 \times 10^5$ is the quality factor of the resonator. In Fig. 2(a), geometry at resonance, and for $n_x = 3 \times 10^{11} \text{ cm}^{-2}$, this leads to $\Delta z_{rms} \simeq 50 \text{ nm}$. Oscillations within these amplitude and frequency ranges have been measured in Ref. 17. The deflection angle $\Delta\Theta$ can then be measured using a deflection-detection (DD) laser and an optical interferometer. We can estimate it²¹ as $\Delta\Theta \simeq L_x L_y \mathcal{F}_{EC} / (12EI)$, where E is the Young's modulus and $I \simeq L_y W^3 / 3$ is the second area moment. Using $E \simeq 80 \text{ GPa}$ for GaAs and $\mathcal{F}_{EC} \simeq 10^{-9} \text{ N}$ for $n_x = 3 \times 10^{11} \text{ cm}^{-2}$, we find that²² $\Delta\Theta \simeq 3 \times 10^{-4} \text{ rad}$.

The created electrons and holes reach thermal equilibrium with the lattice within a few ns. A typical driving pulse in mechanical resonance with the cantilever is 10–20 kHz which is much shorter than the lattice thermalization time and much longer than the exciton lifetime avoiding the heating effects. The resulting resonant amplitude, with the quality factor $Q \simeq 2.5 \times 10^5$ as in Ref. 17, turns out to be about 50 nm as given above.

One should also be aware of another secondary effect, i.e., the photon force exerted by the DD-laser in Fig. 2. If a mW range, 600 nm wavelength is used for the DD-laser, a simple calculation shows that about 10^{-11} N photon force would be exerted on the cantilever at normal incidence which can be reduced by another 10^2 times using a wide angle of incidence. The oscillations of the cantilever are however unaffected by this constant force.

In conclusion, the EC created in a DQW, gives rise to a force that is not known yet in other condensed matter systems. Its existence is supported by the recent conclusive observations of EC.¹⁵ The EC-force, naturally reminds the Casimir effect due to the vacuum fluctuations of the electromagnetic radiation, but its origin is Coulombic although it conceptually differs from the Coulomb force. In the Casimir effect, the driving mechanism is the dependence of the photon density of states on the boundary conditions, whereas in the EC, it is the specific exponential dependence of the Coulomb coupling on the layer separation D . As a result, the EC-force depends on the properties of the condensate. In

particular, the $1/D$ dependence in Eq. (13) is in contrast with the $1/D^4$ dependence of the CF.

Finally, we hope that this work can stimulate research in a broader conceptual perspective where a force due to a quantum condensate can be investigated.

The authors are grateful to K.-J. Friedland (Paul-Drude Institute) and A. Dána (UNAM, Bilkent University), and Nai-Chang Yeh (Caltech) for useful discussions.

¹H. B. G. Casimir, Proc. K. Ned. Akad. Wet. **51**, 793 (1948).

²P. H. G. M. van Blokland and J. T. G. Overbeek, *J. Chem. Soc., Faraday Trans. 1* **74**, 2637 (1978); S. K. Lamoreaux, *Phys. Rev. Lett.* **78**, 5 (1997).

³G. Bressi, G. Carugno, R. Onofrio, and G. Ruoso, *Phys. Rev. Lett.* **88**, 041804 (2002).

⁴V. M. Mostepanenko and N. N. Trunov, *The Casimir Effect and Its Applications* (Oxford Science Publications, 1997); K. A. Milton, *The Casimir Effect* (World Scientific, 2001).

⁵M. E. Fisher and P. G. de Gennes, C. R. Acad. Sci., Paris **B 287**, 207 (1978).

⁶C. Hertlein, L. Helden, A. Gambassi, S. Dietrich, and C. Bechinger, *Nature* **451**, 172 (2008); M. Fukuto, Y. F. Yano, and P. S. Pershan, *Phys. Rev. Lett.* **94**, 135702 (2005); R. Garcia and M. H. W. Chan, *Phys. Rev. Lett.* **88**, 086101 (2002).

⁷S. Biswas, J. K. Bhattacharjee, D. Majumder, K. Saha, and N. Chakravarty, *J. Phys. B* **43**, 085305 (2010); P. A. Martin and V. A. Zagrebnov, *Europhys. Lett.* **73**, 15 (2006).

⁸J. M. Obrecht, R. J. Wild, M. Antezza, L. P. Pitaevskii, S. Stringari, and E. A. Cornell, *Phys. Rev. Lett.* **98**, 063201 (2007); D. M. Harber, J. M. Obrecht, J. M. McGuirk, and E. A. Cornell, *Phys. Rev. A* **72**, 033610 (2005).

⁹S. A. Moskalenko, *Fiz. Tverd. Tela* **4**, 276 (1962); J. M. Blatt, K. W. Ber, and W. Brandt, *Phys. Rev.* **126**, 1691 (1962).

¹⁰M. A. Can and T. Hakioglu, *Phys. Rev. Lett.* **103**, 086404 (2009); T. Hakioglu and M. Sahin, *Phys. Rev. Lett.* **98**, 166405 (2007).

¹¹D. V. Vishnevsky, H. Flayac, A. V. Nalitov, D. D. Solnyshkov, N. A. Gippius, and G. Malpu, *Phys. Rev. Lett.* **110**, 246404 (2013); A. A. High, A. T. Hammack, J. R. Leonard, S. Yang, L. V. Butov, T. Ostatnický, M. Vladimirova, A. V. Kavokin, T. C. H. Liew, K. L. Campman, and A. C. Gossard, *Phys. Rev. Lett.* **110**, 246403 (2013); A. V. Kavokin, M. Vladimirova, B. Jouault, T. C. H. Liew, J. R. Leonard, and L. V. Butov, *Phys. Rev. B* **88**, 195309 (2013).

¹²T. Hakioglu and E. Özgün, *Solid State Commun.* **151**, 1045 (2011).

¹³M. Combescot, O. Betbeder-Matibet, and R. Combescot, *Phys. Rev. Lett.* **99**, 176403 (2007).

¹⁴L. V. Butov, *J. Phys.: Condens. Matter* **16**, R1577 (2004); L. V. Butov, *J. Phys.: Condens. Matter* **19**, 295202 (2007); D. W. Snoke, *Adv. Condens. Matter Phys.* **2011**, 1; D. W. Snoke, *Science* **298**, 1368 (2002).

¹⁵A. A. High, J. R. Leonard, A. T. Hammack, M. M. Fogler, L. V. Butov, A. V. Kavokin, K. L. Campman, and A. C. Gossard, *Nature* **483**, 584 (2012).

¹⁶Including realistic values of m_e and m_h yields a slightly asymmetric shape in the CFE as a function of n_x . Since $n_x = 0$ here, the eh mass difference is not crucial for the physics that follows.

¹⁷H. Yamaguchi, H. Okamoto, S. Ishihara, and Y. Hirayama, *Appl. Phys. Lett.* **100**, 012106 (2012).

¹⁸An important issue here is whether the EC-force can move the sample as a whole instead of the eh wavefunctions within the DQWs. The answer is the strong $E_{ext} \simeq 50 \text{ kV/cm}$ pinning the eh wavefunctions with an external force $F_{ext} \simeq 10^{-6} \text{ N}$. Here, E_{ext} is also necessary in the experiments for promoting the lifetime of the excitons (see Refs. 14 and 15).

¹⁹Here corrections to the \mathcal{F}_C should be considered. A simple calculation yields $\mathcal{F}_C = e^2 n_x^2 A / (2\epsilon) (1 + 2\sqrt{\pi D^2 / A})$. For A and D used here, the finite size correction is about 10^{-3} .

²⁰Using the model in Ref. 12, the ratio of the lifetimes in the upper (u) and the lower (d) quantum wells is given by $\tau_u / \tau_d \simeq |(D_d / D_u) \exp\{-D_d^2 / W_d^2\} / \exp\{-D_u^2 / W_u^2\}|^2$ where $W_d \simeq W_u \simeq 70 \text{ Å}$ as the individual widths of the quantum wells in the upper and the lower DQWs. The widths can be arranged such that $\tau_u / \tau_d \simeq 1$.

²¹I. S. Sokolnikoff, *Mathematical Theory of Elasticity* (Mc Graw Hill, New York, 1956).

²²This is similar to the radian accuracy of the conventional AFMs (10^{-5} rad). [D. A. Bonnelli, D. N. Basov, M. Bode, U. Diebold, S. V. Kalinin, V. Madhavan, L. Novotny, M. Salmeron, U. D. Schwarz, and P. S. Weiss, *Rev. Mod. Phys.* **84**, 1343 (2012)].